Periodica Polytechnica Transportation Engineering

47(3), pp. 178-185, 2019
https://doi.org/10.3311/PPtr.12104

RESEARCH ARTICLE

Implementation of a Robust Electric Brake Actuator Design Based on H-infinity Control Theory

Gábor Péter[1*], György Max[1], Bálint Kiss[1]

Received 15 September 2017; accepted 18 February 2018

Abstract

This paper deals with the robust control system design and implementation of a brake actuator for a smart car. To deliver robust performance, an H_∞ controller had been chosen for the task. This allows excellent disturbance rejection while requiring low computational needs. In order to realize the controller a nominal model of the system has been identified, then, the parameter uncertainties were taken into account to find the stabilizing controller. The brake system consists of a low level H_∞ controller sustaining robustness, a mid-level serial compensator for effective setpoint tracking and a high level supervisory control logic to deliver a reliable system. The implementation was tested and verified on a test bench using rapid prototyping tools and HIL methods.

Keywords

robust control, H-infinity norm, model uncertainty

[1] Department of Control Engineering and Information Technology, Faculty of Electrical Engineering and Informatics, Budapest University of Technology and Economics, H-1521 Budapest, P.O.B. 91, Hungary

[*] Corresponding author, e-mail: petergabor@iit.bme.hu

1 Introduction

Drive-by-wire is the ground version of fly-by-wire which is a standard concept in the aerospace since many years (Stanton and Marsden, 1996). The sole reason it could be adopted in planes is that pilots are well trained compared to car drivers, and larger planes could not be controlled directly by the strength of pilots anyway. In vehicle industry however, the required forces were in a range where human power alone was able to deal with the upcoming requirements. As safety and comfort has always been playing an important role, new driver assistive systems (DAS) were implemented (Isermann et al., 2002) aiming safer and enjoyable driving experience. Recent results show the advances in the field of driver assistive systems (Wang et al., 2013).

The top two safety critical equipment of a car are the steering wheel and the braking system. Both have been updated by servo drives for many years but in different ways. The former uses electrical motors and a control system to deliver an "Optimum steering feel" (Sugitani et al., 1997). The latter utilizes the vacuum produced by the motor to produce a hydraulic amplification. At least it was so until recent years. Nowadays braking systems are also aided by embedded systems where even the pedal position to brake force curve can be adjusted. The evolution of hydraulic brake controllers with embedded systems is still in progress but the results are already exceptional (Aoki et al., 2007).

Servo steering wheels and new generation hydraulic brake controllers enable a driverless experience that is required for autonomous driving. Our research deals with the problem of autonomous driving of cars that are not equipped with such hydraulic modules. Hydraulic amplifiers are employed instead. In these vehicles, the only interface for sending brake commands is the brake pedal itself.

It has to be pressed with fast dynamic and high forces in some cases that make substituting the human driver difficult. Related work of brake by wire system based on nonlinear control theory can be found in (Tanelli et al., 2008). Fuzzy logic fault tolerant control architecture was proposed in (Xiang et al., 2008) that stabilizes the lateral motion of the vehicle. A cooperative method involving the human driver and the assistive system; the based on fuzzy approach is presented in (Nguyen et al., 2015).

This paper details the development of a control loop for an elder car, without the hydraulic controller to enable brake-by-wire concept and thus fully autonomous driving. As the system is fairly unknown and the uncertainties could cause trouble for a simple serial compensator, the H-infinity control method was chosen as robust controller. This type of controller is popular for solving issues with uncertain systems.

In order to cope with the problem of H-infinity theory and integral behavior, a cascade controller including a serial PID compensator and supervisory control logic was designed. The H-infinity controller guarantees robust stability and disturbance attenuation on the lowest level, while the PID-type serial compensator ensures fast and smooth setpoint tracking with no residual error for the whole system.

The paper consists of six sections. Section 2 details the lower levels of the control loop, including speed and position control. Section 3 explains the high level control logic, while Section 4 enlists our experimental results. Finally, the paper is concluded in Section 5.

2 Low-level Cascade Position Control

The system in scope of this design process is a modified brake structure of the RECAR Smart vehicle. In order to deliver the brake-by-wire experience, the vehicle has been heavily modified, new sensors and actuators have been added to support the autonomous functionality.

The hydraulic system behind the pedal is not known thus it is being modelled as uncertainty. The regulations prescribe a sufficient brake force when the pedal is pressed by 500 N and naturally the dynamic should be as high as possible. The fitted electric linear actuator promises a 12 cm/s speed at 500 N force with a steep acceleration ramp even at loaded state. The brake actuator of the RECAR vehicle along with the proposed control loop is depicted in Fig. 1.

The closed loop system relies on two external sensors – one measuring the pedal angle and one measuring the linear actuator displacement – and one internal sensor – as the motor controller hardware can be operated in either current control mode using an internal shunt resistor or in open loop speed control mode.

Fig. 1 RECAR test vehicle and setup

Choosing an optimum control for a given purpose is not a trivial assignment. First, the requirements have to be considered keeping in mind that the system to be controlled might be disrupted in multiple ways. Identifying system parameters could also carry some uncertainty to the system and this could be the source of severe flaws in the final control loop.

For the enlisted reasons a HIL test bench is designed in order to verify the accuracy of the position control to be later used in the RECAR autonomous vehicle. This system consists of a Maxon ESCON 70/10 motor controller and an SKF CATR33H linear actuator including an encoder providing the feedback signal to the Quanser Q8 rapid prototyping hardware.

The motor controller operates in speed control mode (open loop) realizing a simple power stage. The working principle is the following: The PID controller outputs the command speed $\dot{\theta}_c$ and the inner H_∞ loop ensures robust behavior for parameter uncertainties. The outer loop is closed by feeding back the θ position measured with the encoder as depicted in Fig. 2.

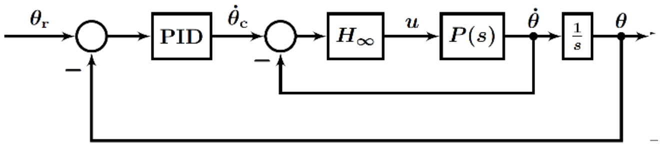

Fig. 2 Cascade control loop

To allow a proper portrayal of the physical process, a plain frequency-domain model of real parametric uncertainty is gauged using real norm-bounded perturbations. The continuous time nominal model of the test bench system is acquired by system identification using Prediction Error Minimization approach (see Fig. 7). A second order process transfer function from input voltage (u) to motor speed ($\dot{\theta}$) is obtained in form of $P_0(s) = A / (s^2 + a_1 s + a_2)$. Then, its worst-case behavior is analyzed by taking into account the variation of each parameter in an interval of ±15 % of its nominal values. Finally, an output multiplicative uncertainty model $P(j\omega)$ is described by

$$P(j\omega) = P_0(j\omega)\left[1 + W_d(j\omega)\Delta(j\omega)\right] \tag{1}$$

$$\left|W_d(j\omega)\right| \geq \max_\omega \left|\frac{P(j\omega) - P_0(j\omega)}{P_0(j\omega)}\right| \quad \forall\omega \tag{2}$$

where $|\Delta(j\omega)| \leq 1$ for all ω represents the normalized real perturbations and $W_d(j\omega)$ is the uncertainty weight upper bounding all error frequency responses resulting from the perturbations.

In order to cope with parameter uncertainties, H_∞ controller structure has been chosen for the lowest level of the controller. H_∞ control methodology is a powerful method in case of uncertain systems, its greatest drawback is the inability to handle systems with pure integrator behavior (Zhou et al., 1996). This problem is solved by separating the control problem into two sub-problems. The low level – speed – controller could be implemented using

H_∞ techniques providing the whole system the required robustness, while the upper level controller could solve the task of a control loop design with pure integrator within.

2.1 H-infinity Robust Speed Control

The low level problem is characterized by the general control structure depicted in Fig. 3, where $G(s)$ denotes the generalized plant model, $w = [d, \dot{\theta}_c]^T$ stands for the exogenous input vector incorporates the speed command signal and disturbance. The control signal is expressed by u and $y = [y_u, y_e]^T$ stands for the controlled output vector, while e denotes the speed error of the motor.

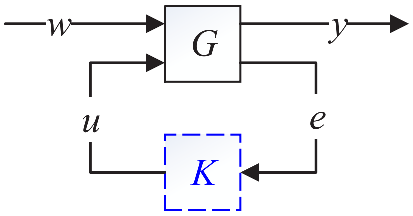

Fig. 3 G-K structure

The design process could be explained as finding a stabilizing controller $K(s)$ for the system $G(s)$ in the manner that according to the information contained by e, the control signal $u = K(s)\,e$ assures internal stability of the closed loop system neutralizes the influence of w on y, thus minimizing the closed loop transfer norm $\|T_{yw}(s)\|_\infty$. Solving this optimization problem is the H_∞ problem that is very difficult to deal with, but the sub-optimal H_∞ problem could be formed and solved if a desired attenuation level γ is selected as in Eq. (3)

$$\| T_{yw}(s) \|_\infty = \| \mathcal{F}_l(G,K) \|_\infty \le \gamma, \tag{3}$$

$$G = \begin{bmatrix} 0 & 0 & W_u \\ W_e P & -W_e M & W_e P \\ -P & I & P \end{bmatrix} = \begin{bmatrix} G_{11} & G_{12} \\ G_{21} & G_{22} \end{bmatrix} \tag{4}$$

where $\mathcal{F}_1(G, K) \triangleq G_{11} + G_{12} K (I - G_{22} K)^{-1} G_{21}$ is the lower linear fractional transformation of systems (G, K).

In other words, the stabilizing controller should deliver a given γ value for amplitude gain of unwanted inputs in the closed loop system in a worst case scenario by taking into account all the uncertainties.

Two weighting sensitivity functions ($W_u(s)$, $W_e(s)$) are included to punish large control signal and discrepancies from nominal system model. The output y_e denotes the weighted difference between the system and the output of reference model $M(s) = \omega_0^2 / (s + \omega_0)^2$, while y_u considers the actuator limitations. Utilizing this set-up, the H_∞ control problem is usually referred to as a weighted mixed sensitivity problem. Therefore, the goal in Eq. (3) is to minimize the effort of the controller and the amplitude of the weighted error signal.

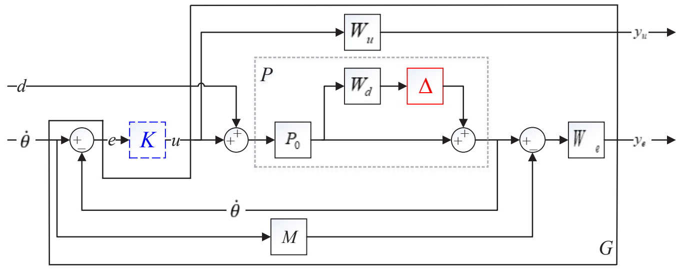

Fig. 4 Internals of G structure

The standard way of solving H_∞ control problems is to use Riccati equations, μ-synthesis or LMI [3, 4]. This results the design of the control law u that is solution of the suboptimal H-infinity problem (3). A bisection algorithm is then used to approach the minimal value of γ. Robust stability (RS) and robust performance (RP) of the H_∞ internally stable control loop then can be tested by the following conditions, see (Zhou and Doyle, 1998):

$$RS \Leftrightarrow \| \mathcal{F}_u\left(G^*, \Delta\right) \|_\infty < 1 \tag{5}$$

$$RP \Leftrightarrow \mu_\Delta(G^*(s)) \triangleq \sup_\omega \mu_\Delta(G^*(j\omega)) < 1 \qquad \omega \in \mathbb{R} \tag{6}$$

where $G^*(s)$ is the resulting system from the standard $\Delta / G / K$ scheme and μ_Δ is structured singular value with respect to Δ.

2.2 PID Position Control

Since $T_{\theta u}(s) = P(s) / s \notin \mathcal{RH}_\infty$, e.g. the transfer function from the input voltage to the motor position is not in the Hardy space of bounded rational functions in the closed right-half plane; H_∞ control synthesis cannot directly be applied for $T_{\theta u}(s)$, for further details see (Zhou et al., 1996). In order to tackle this problem, an outer position control loop, based on PID control algorithm is involved, delivering BIBO stability for the closed-loop system. The construction agenda is as follows. At the beginning, a crossover frequency is chosen based on the plant dynamics, then the parameters of the PID controller are determined for a target phase margin of 60°. Finally, the parameters are finely tuned to achieve decent performance (reference tracking, disturbance rejection) and robustness considering the uncertainties and variations in process dynamics. The resulting transfer function of the PID controller is given by

$$PID(s) = A_p + \frac{A_i}{s} + A_d \frac{N_f s}{s + N_f}, \tag{7}$$

$$A_p = 14.1, \quad A_i = 1.07, \quad A_d = 7.35, \quad N_f = 9.06\,. \tag{8}$$

3 High Level Control Logic

The high level state machine (High Level Control Logic) is in charge of supervising the whole brake system. The supervisory logic has been implemented as an embedded Matlab Function with two adjustable parameters:

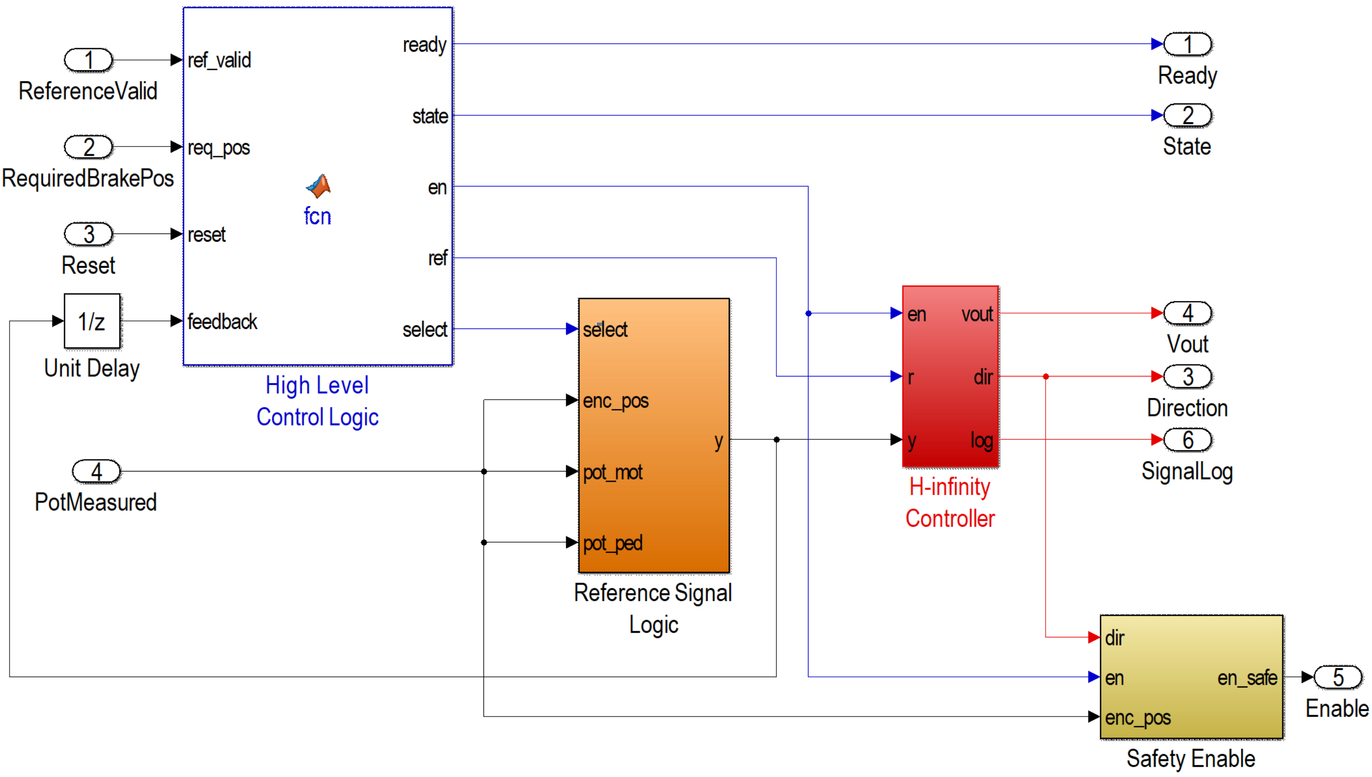

Fig. 5 Block diagram of the controller

1. *pot_mot_emergency_setpoint*: Position constant of the emergency wind up mechanism (given in mm)
2. *pot_mot_relaxed*: Relaxed position constant of the actuator (given in mm).

The latter position could be treated as zero position throughout normal operation of the system. The system is shown in Fig. 5. As the application is critical (braking), the supervisory control can override the control signal of the controller if it detects any invalidity. This is realized by the Safety Enable block on the block diagram.

The state machine of the high level control is depicted in Fig. 6. It has the following principle of operation:

- After startup, the machine resides in *State 0*, waiting for a *Reset* signal.
- As soon as the *Reset* signal is present the machine progresses to *State 1* and commences the windup sequence. After successfully accomplishing the safety critical task, the machine jumps to the next state, *State 2*.

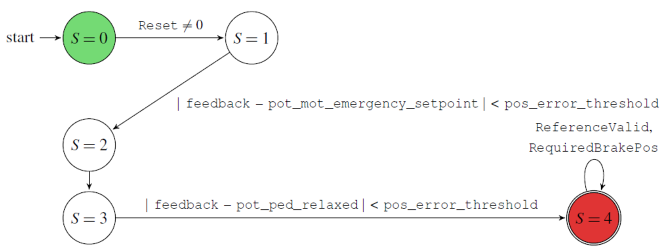

Fig. 6 High Level Control Logic: State machine

- In *State 2*, the machine selects the appropriate feedback sensor according to the configuration file, then switches to *State 3* automatically.
- In *State 3*, the machine orders the controller to finish the windup process by setting the relaxed position as setpoint. As soon as the relaxed position is reached, the system is ready for normal operation thus it slides to the active state denoted as *State 4*.
- While in *State 4* (Normal operation), the low level controller holds the pedal at *RequiredBrakePos* position as long as the *ReferenceValid* signal is valid. Should the *ReferenceValid* signal fade into invalid, the controller forces the pedal back to relaxed position.

4 Experimental Results

The control design has been tested on a real system using HIL methods. The first step was obtaining a nominal transfer function $P_0(s)$ for the system. This was achieved by sending out an identification signal (Voltage) to the Maxon motor controller and measuring the feedback signal (Speed). As position is the integral of speed, the transfer function from motor controller hardware input signal (Voltage) to position arises in a single step.

Practical identification needs some tweaking as encoders deliver position instead of speed. The result of identification is depicted in Fig. 7.

Perturbing all three parameters by ±15 % resulted in different step responses as displayed in Fig. 8. The figure shows the response of all 28 slightly modified systems and of the nominal system as well (1 lagged and 27 perturbed systems).

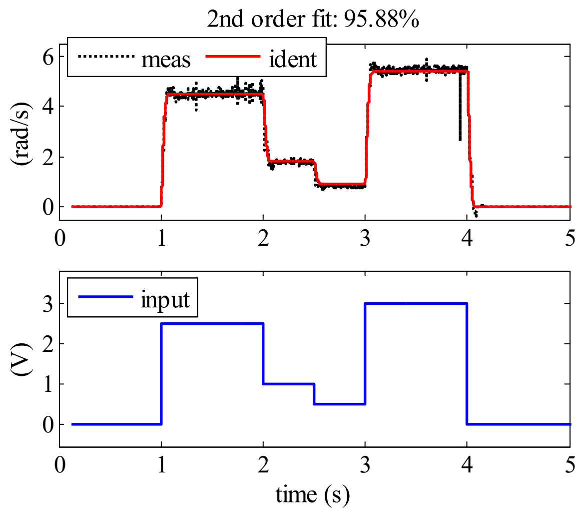

Fig. 7 Identification of plant model

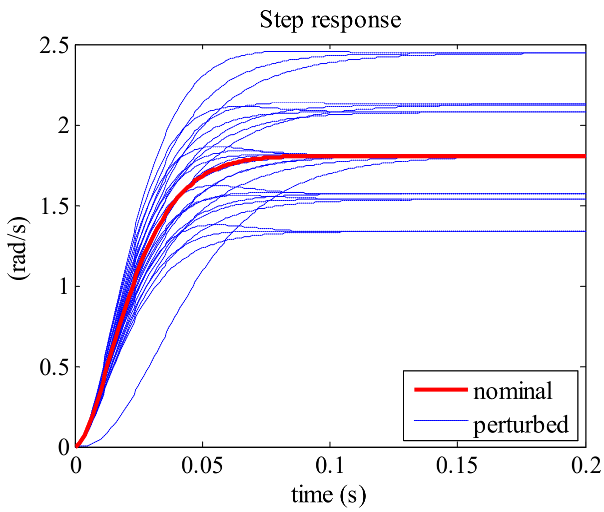

Fig. 8 Step responses of nominal and perturbed systems

4.1 Low Level

Solving the H_∞ (suboptimal) problem requires the wrapper function $W_d(j\omega)$ which depicts a worst case scenario throughout the whole frequency spectrum including all the 28 systems. To visualize this curve, an amplitude plot is displayed in Fig. 9, including the frequency response of all systems in blue and the wrapper function in red.

After choosing the wrapper function and obtaining a stabilizing controller K as described in Section 2, the next step was testing the perturbed systems and the real system with the controller. The step responses including disturbance rejection are depicted in Fig. 10. The amplitude of the disturbance almost equals the amplitude of the step function, but the H_∞ controller assures robustness, while the serial PID compensator ensures fast setpoint tracking.

The bottom subfigure visualizes the setpoint change and the disturbance over time. The top subfigure displays the output of different systems receiving the same setpoint change and disturbances mentioned above. The motor position of the real system is depicted with a black dashed line, while the other lines

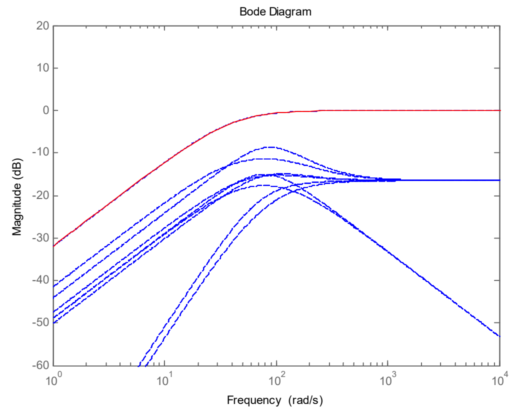

Fig. 9 Amplitude plots including function $W_d(j\omega)$

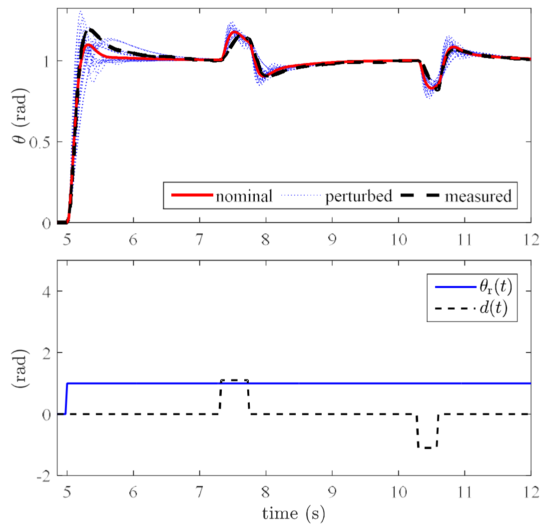

Fig. 10 Step response in closed loop

represent simulation results. The nominal plant is illustrated with a solid red line, having almost identical curves as the real system. Parameter perturbed outputs are depicted with grey dotted lines, having similar transients to the nominal system.

The corresponding controller command signals are depicted in Fig. 11. The control signal (u) and motor speed ($\dot{\theta}_c$) are shown on the right, demonstrating close-to-real behavior and applicable limits in case the measured and the perturbed systems.

4.2 Full System

The effectiveness of the proposed cascade control scheme is evaluated on the prototype hardware system. Using the following weighting functions,

$$W_u(s) = \frac{0.005(0.001s + 0.01)}{0.05s + 1}, \tag{9}$$

$$W_e(s) = \frac{0.5(2s + 1)}{2s + 0.01}, \tag{10}$$

the H_∞ control problem has a solution for γ_{min} = 0.507. An order reduction procedure, based on the controller's Hankel singular values (Zhou and Doyle, 1998), is then applied on the synthetized 9th order controller to achieve a 3rd order

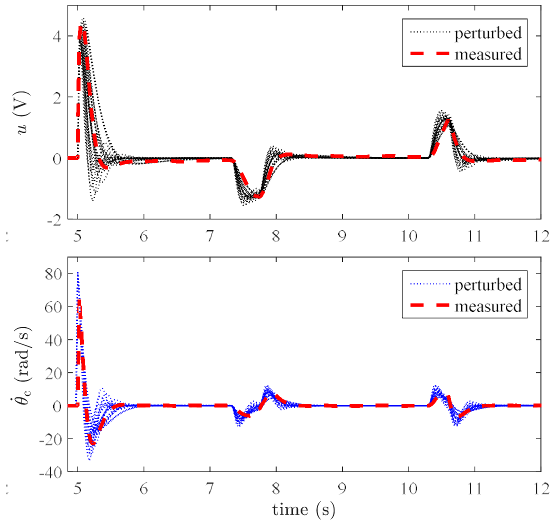

Fig. 11 H-infinity (top) and PID (bottom) control signals of prototype system

transfer function allowing its practical implementation on the AutoBox HIL system.

Two scenarios were investigated on the RECAR vehicle and the whole hardware system including supervisory control. Fig. 12 displays the test results of Scenario 1. The requested position (30 mm) is constant over time and the actual position changes as the initial sequence runs after the reset signal.

After the emergency setpoint is reached, the control system pulls the brake pedal back to its relaxed position. At $t = 2$ seconds, a reference valid signal appears, indicating a possible braking action, i.e. a new setpoint to the system. The position change takes place in around 200 milliseconds and 100 mm/s peak velocity. The next action is triggered on the falling edge of the reference valid signal as the controller sets the output position back to the relaxed position in another 200 milliseconds.

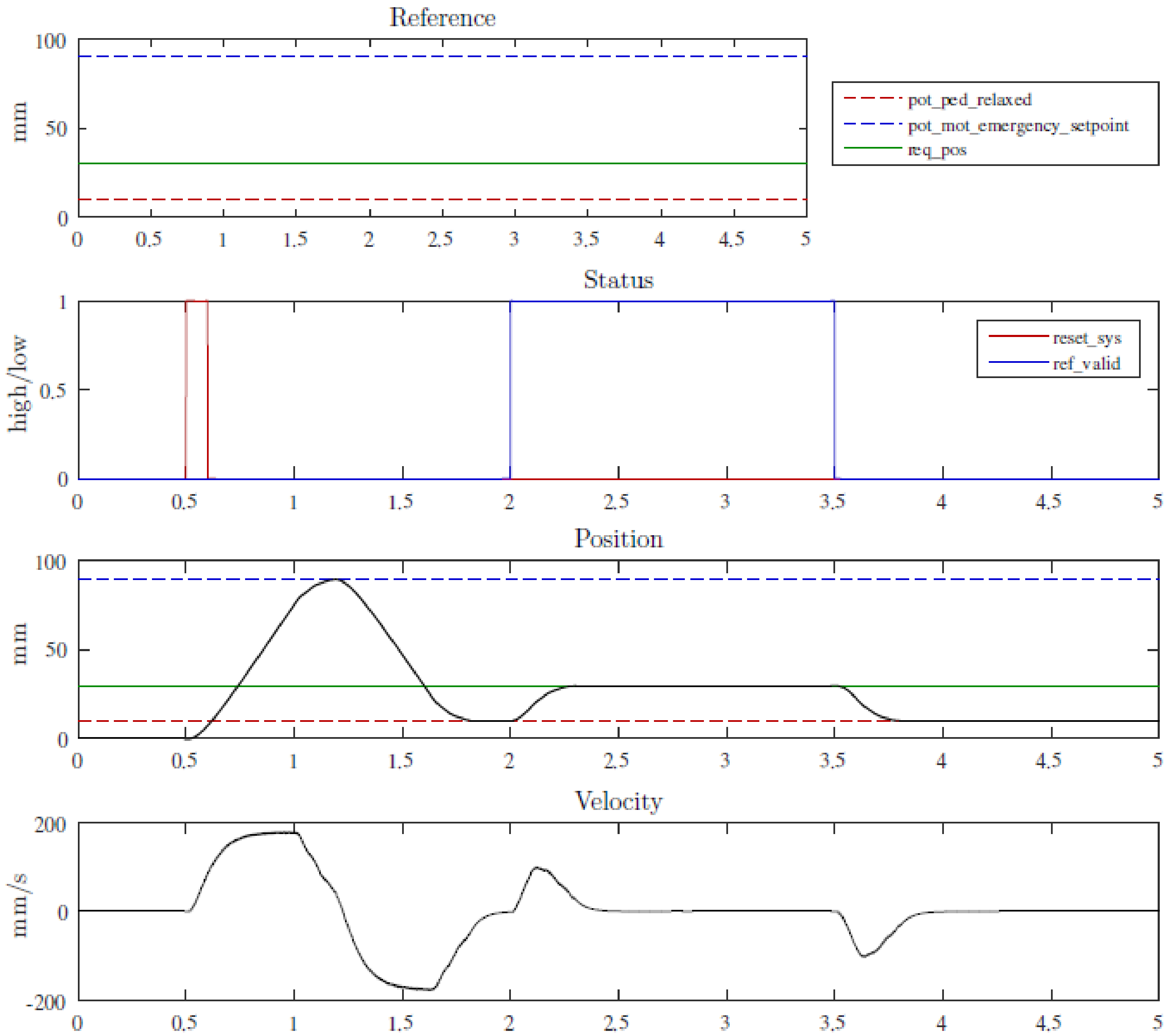

Fig. 12 Signals: Scenario 1

Fig. 13 shows the input and output signals of Scenario 2, where the reference valid signal is true for only a short period of time, thus the brake pedal could not reach the desired position of 50 mm. It can be observed that the peak velocities are around 180 mm/s satisfying the control objectives in this case as well.

5 Conclusion

The selected cascade H_∞ / PID method proved to be useful for realizing a robust position control scheme according to the simulations and experimental measurements carried out on the RECAR autonomous vehicle. Stability is guaranteed even at high model parameter uncertainties resulting in an agile control loop.

The braking system is extended with a high level control logic unit which allows supervisory actions by employing state machine. Such actions are the initial validation of emergency braking and monitoring for any invalidity.

Future work will include the development of an autonomous traffic cruise control system to enable convenient cruising experience for the passengers.

Acknowledgement

The project has been supported by the European Union, co-financed by the European Social Fund. EFOP-3.6.2-16-2017-00002.

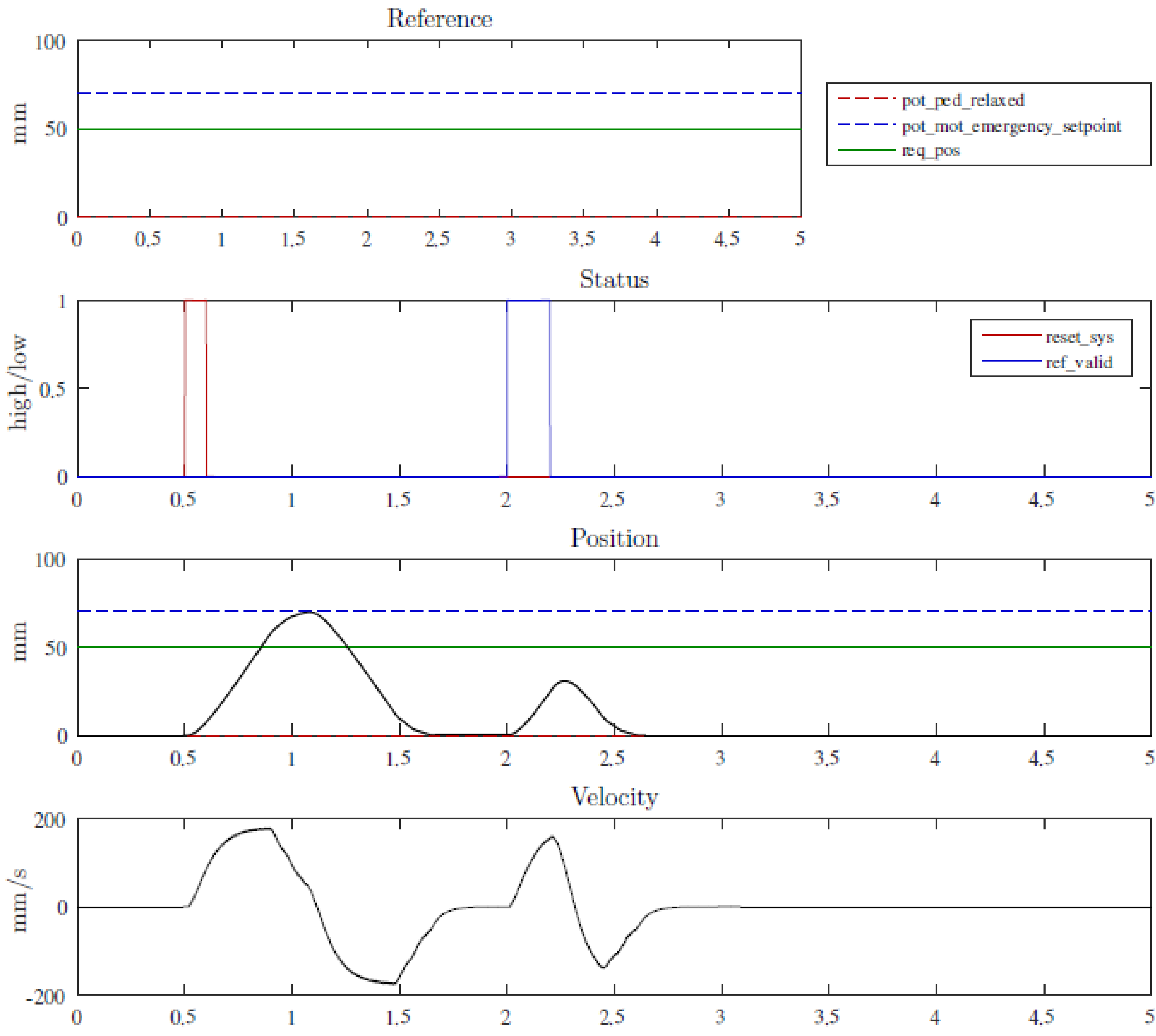

Fig. 13 Signals: Scenario 2

References

Aoki, Y., Suzuki, K., Nakano, H., Akamine, K., Shirase, T., Sakai, K. (2007). Development of Hydraulic Servo Brake System for Cooperative Control with Regenerative Brake. SAE Technical Paper 2007-01-0868. http://doi.org/10.4271/2007-01-0868

Isermann, R., Schwarz, R., Stolzl, S. (2002). Fault-tolerant drive-by-wire systems. *IEEE Control Systems Magazine.* 22(5), pp. 64–81. http://doi.org/10.1109/mcs.2002.1035218

Nguyen, A.-T., Sentouh, C., Popieul, J.-C., Soualmi, B. (2015). Shared lateral control with on-line adaptation of the automation degree for driver steering assist system: A weighting design approach. In: *2015 IEEE 54th Conference on Decision and Control (CDC)*. Osaka, Japan, Dec. 15-18., 2015. pp. 857-862. http://doi.org/10.1109/cdc.2015.7402336

Stanton, N. A., Marsden, P. (1996). From fly-by-wire to drive-by-wire: Safety implications of automation in vehicles. *Safety Science.* 24(1), pp. 35–49. http://doi.org/10.1016/s0925-7535(96)00067-7

Sugitani, N., Fujuwara, Y., Uchida, K., Fujita, M. (1997). Electric power steering with H-infinity control designed to obtain road information. *Proceedings of the 1997 American Control Conference* (Cat. No.97CH36041). http://doi.org/10.1109/acc.1997.611995

Tanelli, M., Astolfi, A., Savaresi, S. M. (2008). Robust nonlinear output feedback control for brake by wire control systems. *Automatica.* 44(4), pp. 1078–1087. http://doi.org/10.1016/j.automatica.2007.08.020

Wang, J., Zhang, L., Zhang, D. (2013). An Adaptive Longitudinal Driving Assistance System Based on Driver Characteristics. *IEEE Transactions on Intelligent Transportation Systems.* 14(1), pp. 1–12. http://doi.org/10.1109/tits.2012.2205143

Xiang, W., Richardson, P. C., Zhao, C. (2008). Automobile Brake-by-Wire Control System Design and Analysis. *IEEE Transactions on Vehicular Technology.* 57(1), pp. 138–145. http://doi.org/10.1109/tvt.2007.901895

Zhou, K., Doyle, J. C., Glover, K. (1996). Robust and Optimal Control. Prentice Hall, New Jersey, USA.

Zhou, K., Doyle, J. C. (1998). Essentials of Robust Control. Prentice Hall, Upper Saddle River, New Jersey, USA.